Chemical Engineering Journal 172 (2011) 277–286

Contents lists available at ScienceDirect

Chemical Engineering Journal

journal homepage: www.elsevier.com/locate/cej

Equilibrium and kinetic studies on removal of Cu^{2+} and Cr^{3+} from aqueous solutions using a chelating resin

Licínio M. Gando-Ferreira*, Inês S. Romão, Margarida J. Quina

Centre for Chemical Processes Engineering and Forest Products (CIEPQPF), Department of Chemical Engineering, University of Coimbra, Pólo II, Rua Sílvio Lima, 3030-790 Coimbra, Portugal

ARTICLE INFO

Article history:
Received 14 April 2011
Received in revised form 28 May 2011
Accepted 30 May 2011

Keywords:
Ion-exchange equilibrium
Separation Cu^{2+}/Cr^{3+}
Chelating resin Diaion CR 11
Breakthrough curves
Regeneration

ABSTRACT

In this study, a chelating resin, Diaion CR 11, was studied in order to selectively remove Cu^{2+} and Cr^{3+} present in synthetic effluents. Single-component equilibrium isotherm was determined in batch experiments for copper, and an exchange equilibrium based model was used to correlate the experimental data of the binary system Cu^{2+}/H^+. It was observed that the maximum capacity of the resin increased 2.3 times when the pH varied from 2 to 5 at 25 °C. The equilibrium constant increased 1.4 times when the temperature changed from 25 to 50 °C at initial pH of 3. For the operating conditions tested, it was found that the resin exhibited a better selectivity for Cu^{2+} over Cr^{3+}. A mathematical dynamic model was successfully implemented for describing the saturation behavior of the multicomponent system $Cu^{2+}/Cr_t/H^+$ in the column operation. The regeneration of the resin was also experimentally studied by using HCl followed by a mixture of $NaOH/H_2O_2$. High efficiencies were observed for copper during the first step, where it was almost fully eluted from the resin with 1 M HCl. The use of those regenerant agents in the presence of iron seems to effectively strip chromium from the resin.

© 2011 Elsevier B.V. All rights reserved.

1. Introduction

The environmental contamination with heavy metals may create acute or chronic toxicity problems, which should be avoided whenever possible. Indeed, although heavy metals could be found naturally in soils, sediments, water and even in living organisms, anthropogenic releases can increase its concentration to unacceptable levels [1,2]. The electroplating industries are examples of processes that may create serious problems, since their wastewaters may contain large number of heavy metals, including chromium, copper, nickel, zinc, manganese and lead [3]. The specific contaminants addressed in our work were chromium and copper. Chromium was selected mainly due to its high concentration in electroplating effluents, significant commercial value and also based on health concerns. In fact, chromium may be regarded as a very toxic non-essential metal for microorganisms and plants, being well known that hexavalent form is significantly more toxic than the fairly innocuous and less mobile trivalent form [4,5]. Adverse effects of chromium on plants may be observed during germination processes, growth of roots, stems and leaves, as well as throughout plant physiological processes such as photosynthesis, water relations and mineral nutrition [5]. Copper is in general a heavy metal of concern because of its toxicity to aquatic life [6]. For instance, although normal growth of most plants occurs at 5–20 mg L^{-1}, they may suffer from copper deficit at concentrations below 5 mg L^{-1} or from Cu^{2+} toxicity at concentrations over 20 mg L^{-1} [1]. Also Babula et al. stressed that Cu^{2+} may be essential as constituent of pigments and enzymes but it becomes toxic at high concentration because of disrupting enzyme functions, replacing essential metals in pigments or producing reactive oxygen species [7].

Intended for removal and recovery of valuable metals, ion exchange has been recognized as a promising alternative technique to traditional methods of precipitation coupled with filtration. The chelating resins are commonly employed as ion-exchange materials, once their ligands can selectively bind to certain metallic ions through ionic and coordinating interactions. Recent studies have shown that these resins could be used for selective removal and recovery of chromium and copper [3,8–18]. The pH, metal concentration and temperature are the key variables that influence the performance of ion exchange process. Gode and Pehlivan [12] studied the effect of these variables on sorption of Cr^{3+} into macroporous resins containing iminodiacetic acid (Lewatit TP 207 and Chelex-100), and observed that the maximum sorption occurs at pH 4.5 and a slight raise in the equilibrium constant as temperature increases. Pehlivan and Altun [10] reported an optimum pH range of 4.5–5.5 for the sorption of Pb^{2+}, Cu^{2+}, Zn^{2+}, Cd^{2+}, and Ni^{2+} on Lewatit TP 207 (weakly acidic and chelating resin). Lin and Juang

* Corresponding author. Tel.: +351 239 798700.
E-mail address: lferreira@eq.uc.pt (L.M. Gando-Ferreira).

1385-8947/$ – see front matter © 2011 Elsevier B.V. All rights reserved.
doi:10.1016/j.cej.2011.05.105

[11] tested two chelating resins (Chelex 100 and Amberlite IRC-748) in the Na^+ form for the exchange Cu^{2+}/Zn^{2+} by varying the initial concentration (3–9 mol m^{-3}) and the solution pH (2–6.5). Yalçin et al. [17] proposed a combined treatment for the recovery of copper and chromium from electroplating effluents. They used the chelating resin Amberlite IRC-718 for uptaking Cu^{2+} from alkaline baths containing cyanide that were first subjected to oxidation and neutralization. Chromium trivalent was recovered by Amberlite IRC-50 (weakly acidic resin) and eluted with H_2O_2 and NaOH.

The equilibrium data reported in literature are often empirically correlated with conventional isotherm equations, such as Langmuir, Freundlich and other [9,10,12,19,20]. In our work, the ion-exchange equilibrium data were described with a suitable model that takes into account the effect of operating variables, such as pH, on the resin selectivity, as well as the speciation of species in solution. This information is important to study the dynamics of the ion-exchange process in fixed-bed through the application of a mathematical model that can successfully predict experimental breakthrough curves at different operating conditions. The regeneration step of the resin is a key issue in the evaluation of global performance process for selective recovery of metals. Few studies were found in the literature on the regeneration of resins pre-saturated with copper and especially with trivalent chromium. The use of conventional acidic or alkaline chemicals for striping chromium from cationic resins does not enable to obtain acceptable levels of efficiency [3,21]. As alternative, the oxidative elution can be a good solution where the retained Cr^{3+} is converted to CrO_4^{2-} anion that is rejected by the resin. Petruzzelli et al. [21] tested different regeneration protocols for striping Cr^{3+} from a macroporous carboxylic resin. They developed the IERECHROM process where aluminum and chromium were separated and the latter in the form of chromate by using as regenerant agent the mixture $NaOH/H_2O_2$.

In this study, ion exchange equilibrium data using a chelating resin, Diaion CR 11, for the binary system Cu^{2+}/H^+ was studied in detail giving a particular emphasis to the effects of initial pH and temperature on the resin's selectivity. Moreover, the dynamic behavior of the saturation and regeneration steps in fixed-bed with multicomponent mixtures of copper and chromium was as well investigated. It is worth mentioning that exchange data between heavy metals and the resin tested in this work are very limited in literature.

2. Theory

2.1. Equilibrium model

The resin used contains a functional group of iminodiacetic type with two protons available that exhibits large affinity for alkaline earth and transition metal ions. The order of selectivity for some metals in solution is as follows: $Fe^{3+} > Al^{3+} > Hg^{2+} > Cu^{2+} > Pb^{2+} > Ni^{2+} > Cd^{2+} > Zn^{2+} > Co^{2+} > Mn^{2+} > Ca^{2+} > Mg^{2+}$ [22]. The general equation for describing the binary ion-exchange equilibrium of divalent metals ions with an iminodiacetic resin can be represented by:

$$nR - H_r + M^{2+} \leftrightarrow R_{(nr-s)} - M^{(nr-s)} + sH^+ \quad (1)$$

where $n = 1$, $r = 2$ and $s = 1$ or 2, M^{2+} refers to a divalent metal ion, $nR - H_r$ correspond to the free resin sites and $R_{(nr-s)} - M^{(nr-s)}$ to the metal complexed on the resin.

Our studies, performed in order to evaluate the experimental equilibrium data involving Cu^{2+} and the resin Diaion CR 11, led to the conclusion that the most likely chemical reaction of exchange is, as follows ($s = 1$):

$$RH_2 + M^{2+} \leftrightarrow RHM^+ + H^+ \quad (2)$$

Considering that the activity coefficients for both phases are equal to unity (condition of ideality), the equilibrium constant can be written as:

$$K_{M,H} = \frac{[RHM^+][H^+]}{[RH_2]\left[M^{2+}\right]} \quad (3)$$

The molar concentrations of the species in Eq. (3) can be substituted by the quotient between normality and respective valence coefficient. On the other hand, the equivalent fractions for each species in solid phase, Y_i, and liquid phase, X_i, can be defined as:

$$Y_i = \frac{q_i}{q_{\max}}, \quad X_i = \frac{C_i}{C_T} \quad (i = 1 - M \text{ and } 2 - H); \quad C_T = C_{H^+} + C_{M^{2+}} \quad (4)$$

where q_i is the amount of metal ion exchanged (meqv g^{-1}_{resin}), q_{max} the total operating capacity of the resin (meqv g^{-1}_{resin}), $C_{M^{2+}}$ and C_{H^+} are the concentrations of metal and hydrogen ion in solution expressed in meqv L^{-1}. Since the summations of the equivalent fractions of the metal and hydrogen in the solution and resin phases are both equal to unity, Eq. (3) becomes

$$Y_M = \frac{K_{M,H} X_M}{1 + (K_{M,H} - 1) X_M} \quad (5)$$

The description of ion-exchange equilibrium data through Eq. (5), in which the ionic fraction of metal in the resin can be calculated as function of its ionic fraction in solution, requires that the chemical species of metal in aqueous solution are known. The distribution of the copper and chromium species at different pH values was evaluated by using visual MINTEQA2 software, which is a free computer program for chemical speciation calculations.

During experiments involving the exchange of copper and chromium on the resin Diaion CR 11, in the H^+ form, it was observed that the equilibrium pH's are always lower than 3.5. Then, according to the speciation data in copper salt solutions, Cu^{2+} is the predominant specie (near 100%). In the case of solutions of trivalent chromium, the species in solution are Cr^{3+}, $Cr(OH)^{2+}$ and $Cr(OH)_2^+$. The ionic specie Cr^{3+} represents 84.4% in a solution at a pH 3 whilst at a pH 2 this amount increases to 98.3%. Hence, it is very probable that chelation occurs between Cr^{3+} ion and the iminodiacetic group of the resin. To calculate the concentration of this species in solution, the following equilibrium reactions were considered, which are characterized by the equilibrium constants K_1 and K_2 [23].

$$Cr^{3+} + H_2O \leftrightarrow Cr(OH)^{2+} + H^+ \quad pK_{1(T=25C)} = 3.85 \quad (6)$$

$$Cr^{3+} + 2H_2O \leftrightarrow Cr(OH)_2^+ + 2H^+ \quad pK_{2(T=25C)} = 10.06 \quad (7)$$

The total solution concentration of chromium, $C_{Cr,t}$ is

$$C_{Cr,t} = C_{Cr^{3+}} + C_{Cr(OH)^{2+}} + C_{Cr(OH)_2^+} \quad (8)$$

By solving simultaneously the equations that define the equilibrium constants K_1 and K_2, Eqs. (6) and (7), together with Eq. (8), the concentration of Cr^{3+} in solution is obtained through Eq. (9):

$$C_{Cr^{3+}} = \frac{C_{Cr,t} C_{H^+}^2}{C_{H^+}^2 + K_1 C_{H^+}^2 + K_2} \quad (9)$$

The equilibrium constant for the binary system Cu^{2+}/H^+, $K_{Cu,H}$, will be estimated by fitting Eq. (5) to the experimental data. The approach based on Eqs. (6)–(9) will be used for predicting the multicomponent ion-exchange equilibrium $Cu^{2+}/Cr^{3+}/H^+$ in the dynamic behavior of the saturation step in column.

2.2. Dynamic model for fixed-bed sorption process

A dynamic model was used for describing the sorption behavior of the Cu^{2+} and Cr^{3+} onto Diaion CR 11 in a fixed-bed system. This model considers negligible the electrical field effect and includes

the mass balance in liquid phase, the ion-exchange equilibrium relationships and the mass transfer inside the particles (intraparticle) given by a linear driving force (LDF) rate [24]. The resistance to mass transfer across the film fluid-particle was neglected. Accordingly, the dimensionless model equations are:

2.2.1. Mass balance for the fluid phase

$$\frac{\partial x_i(z*,\theta)}{\partial\theta} = \frac{1}{Pe}\frac{\partial^2 x_i(z*,\theta)}{\partial z*^2} - \frac{\partial x_i(z*,\theta)}{\partial z*} - \frac{(1-\varepsilon)}{\varepsilon}\rho_h \frac{q_{\max}}{C_{E_i}}\left(\frac{\partial Y_i(z*,\theta)}{\partial\theta}\right) \quad (10)$$

where $i=1$ for Cr_t and 2 for Cu^{2+}; $x_1 = C_1/C_{1E}$ and $x_2 = C_2/C_{2E}$ are the normalized concentrations of total chromium and ion copper in the bulk liquid phase; $\theta = t/\tau$ is the reduced time, τ is the bed space time; $z^* = z/L$ is the reduced axial coordinate, L the bed length; $Pe = uL/(\varepsilon D_{ax})$ is the dimensionless group Peclet number, where D_{ax} is the axial dispersion coefficient, and ρ_h is the wet density of the resin. All the symbols included in Eq. (10) are fully listed in the nomenclature.

2.2.2. Intraparticle mass transfer

$$\frac{\partial Y_i(z*,\theta)}{\partial\theta} = \tau K_{\mathrm{LDF}_i}(Y_i^*(z*,\theta) - Y_i(z*,\theta)) \quad (11)$$

where K_{LDF_i} is the LDF kinetic constant and $Y_i^*(z*,\theta)$ is the equivalent fraction of metal i adsorbed on the resin in equilibrium with the bulk concentration.

2.2.3. Multicomponent ion-exchange equilibrium model

$$K_{i,H} = \frac{Y_i^*(1-X_1-X_2)}{(1-Y_1^*-Y_2^*)X_i} \quad (12)$$

$$X_1 = \frac{C_{Cr^{3+}}}{C_{Cr^{+3}} + C_{Cu^{2+}} + C_{H^+}}, X_2 = \frac{C_{Cu^{2+}}}{C_{Cr^{3+}} + C_{Cu^{2+}} + C_{H^+}} \quad (13)$$

where $C_{Cr^{3+}}$ and $C_{Cu^{2+}}$ are the concentrations of Cr^{3+} and Cu^{2+} in the bulk solution expressed in meqv L^{-1}. Note that an exchange reaction for the binary system Cr^{3+}/H, described by Eq. (2), was assumed.

The hydrogen ion concentration, C_{H^+}, may be calculated from the electroneutrality condition:

$$C_{Cr^{3+}} + C_{Cr(OH)^{2+}} + C_{Cr(OH)_2^+} + C_{Cu^{2+}} + C_{H^+} = C_{OH^-} + C_{NO_3^-} \quad (14)$$

where C_{OH^-} is the concentration of hydroxyl ion, given by the dissociation product of water, K_w, and $C_{NO_3^-}$ the concentration of nitrate species. The co-ion (NO_3^-) should be excluded from the resin due to the Donnan effect, thus its concentration remains constant in all the experiments.

Considering the definition of the equilibrium constants for the hydrolysis reactions of trivalent chromium in aqueous solution (Eqs. (6) and (7)), the electroneutrality equation may be expressed as

$$C_{Cr^{3+}} + \frac{K_1 C_{Cr^{3+}}}{C_{H^+}} + \frac{K_2 C_{Cr^{3+}}}{C_{H^+}^2} + C_{Cu^{2+}} + C_{H^+} = \frac{K_w}{C_{H^+}} + C_{NO_3^-} \quad (15)$$

in which the concentration of Cr^{3+} is calculated with Eq. (9).

2.2.4. Boundary conditions

$$z^* = 0 \quad x_i(z^*,0) = 1 \quad (16)$$

$$z^* = 1 \quad \left.\frac{\partial x_i(z^*,\theta)}{\partial z^*}\right|_{z*=1} = 0 \quad (17)$$

2.2.5. Initial conditions

$$\theta = 0 \quad x_i(z^*,0) = 1; \quad x_i(z^*,\theta>0) = 0 \quad (18)$$

The axial dispersion, D_{ax}, included in the Peclet number was calculated from the Butt correlation [25]:

$$\left(\frac{ud_p}{D_{ax}}\right) = (0.2 + 0.011Re^{0.48}), \quad \text{where } Re = \frac{u\rho d_p}{\varepsilon\mu} \quad (19)$$

accordingly, its value in the model was 2.15×10^{-6} m^2/s. The linear driving force K_{LDF} was estimated by the following expression:

$$K_{LDF_i} = \frac{15D_{ei}}{R_p^2\rho_h\left(\frac{dq_i^*}{dC_i}\right)} \quad (20)$$

where D_{ei} is the effective pore diffusivity of species i, R_p is the radius of the particle, dq_i^*/dC_i is the gradient of the equilibrium data, and $q_i^* = q_{\max}Y_i^*$.

The D_e for copper ion was estimated from the equation:

$$D_e = \frac{\varepsilon_p D_m}{\tau_p} \quad (21)$$

in which D_m is the molecular diffusivity of the ion metal in water, τ_p the tortuosity factor, estimated by $1/\varepsilon_p$ [26], and ε_p the internal porosity of the resin. The molecular diffusivity expressed in m^2 s^{-1}, may be estimated in this case by the Nernst equation that depends on the equivalent ionic conductance λ of the metal in solution [27]:

$$D_m = 2.661\times10^{-11}\frac{\lambda}{|Z|} \quad (22)$$

where Z is the valence of the ion.

The effective pore diffusivity for copper ion, calculated through Eq. (21), was of 3.08×10^{-10} m^2/s. For chromium, the balance equations take into account the total concentration of all species involved in the speciation equilibrium, Cr_t, and thus Eq. (22) is not valid for estimating the diffusivity coefficient of this species. In this case, the effective pore diffusivity for chromium was considered an adjustable parameter of the model. In short, the parameters incorporated in the model are $D_{eCr,t}$, $k_{Cr,H}$ and $k_{Cu,H}$ which were estimated by fitting the model solution to experimental saturation curves. The model equations Eqs. (10)–(18) were numerically solved with the PDECOL package [28].

3. Experimental

3.1. Resin and chemicals

The cationic resin Diaion CR 11 resin used in this study was supplied by Sigma–Aldrich, and it contains iminodiacetic group as chelating ligand which is bonded onto a crosslinked polystyrene matrix. Before the experiments, the resin was pretreated by cyclic washings with 2 M HCl and 2 M NaOH solutions used for removing solvents and other preparation chemicals. The last step of the resin conditioning consisted in percolating a solution of HCl through the resin in order to convert it into H^+ form.

Synthetic effluent samples were prepared by dissolving an appropriate amount of chromium salt, $Cr(NO_3)_3$, and copper salt, $Cu(NO_3)_2$, in distilled water. All the chemicals used were of analytical grade and supplied by Ridel-de-Haën.

3.2. Physical characterization of resin

Several physical properties of the Diaion CR 11 resin were assessed experimentally. The real density, ρ_r, and wet density, ρ_h, were evaluated by the displacement of n-heptane in a picnometer. The moisture content, H (%), was determined by gravimetry after drying resin samples at 80 °C. The apparent density, ρ_{ap}, and

Table 1
Experimental conditions of saturation and regeneration experiments in fixed-bed column.

Run	T (°C)	Feed pH	$C_{Cr,t}$ (meqv L^{-1})	$C_{Cu^{2+}}$ (meqv L^{-1})	C_{NO_3} (meqv L^{-1})
Saturation step					
1	25	3.25	13.27 (230[a])	10.86 (230[a])	22.0
2	25	3.11	13.27 (230[a])	3.30 (70[a])	17

Run	T (°C)	Initial pH	C_{HCl} (mol L^{-1})	C_{NaOH/H_2O_2} (mol L^{-1})
Regeneration step				
3	25	2.72	1	2/0.15
4	50	2.72	1	2/0.15
5	50	2.72	1	2/0.30
6[b]	25	2.82	1	2/0.33

Bed properties and flow conditions: interparticle porosity, $\varepsilon \approx 0.40$; bed length, $L = 10$ cm; flow rate, $Q = 10\ cm^3\ min^{-1}$; intraparticle porosity, $\varepsilon_p = 0.66$; particle radius, $R_p = 2.60 \times 10^{-2}$ cm [3]; wet density, $\rho_h = 1.015\ g\ cm^{-3}$; maximum exchange capacity, $q_{max} = 1.3$ meqv g^{-1}.
[a] mg L^{-1}.
[b] Resin pre-saturated with 464 mg L^{-1} of Cr_t.

particle porosity, ε_p, were calculated by the following equations, respectively: $\rho_{ap} = (1 - H/100)\rho_w$ and $\varepsilon_p = 1 - \rho_{ap}/\rho_r$. FT-IR spectra were recorded with a Jasco FT/IR 4200 spectrometer, resolution 2 cm^{-1}, in the range of 4000–400 cm^{-1} by KBr pellet technique.

3.3. Equilibrium experiments

Equilibrium isotherms for the binary system Cu^{2+}/H^+ were determined through batch tests, where 40 mL of a synthetic solution of known pH and composition were added into several flasks containing different amounts of preconditioned resin. The flasks were sealed and kept in a shaker at constant temperature (25 or 50 °C) for 24 h. At the end of this period, the resin was separated by filtration and aliquots of liquid were chemically analyzed. Initial pH 2, 3 and 5 were pre-adjusted by a few drops of HNO_3 or NaOH. The metal content was analyzed by flame atomic absorption spectrophotometry, PerkinElmer 3300. The pH measurement was carried out potentiometrically using a WTW pH meter, Inolab level.

3.4. Fixed-bed experiments

In the column tests, a glass tube with 1.6 cm of internal diameter and 20 cm height, packed with approximately 7–8 g of resin was used. A peristaltic pump was utilized to percolate 10 mL/min of a synthetic or industrial solution containing metal ions through the column during the saturation step. The regeneration experiments of pre-saturated resin were sequentially performed using 1 M HCl followed by $NaOH/H_2O_2$ solution. Several samples were collected at the column outlet and the concentrations of the metals were analyzed along the time as described above. The conditions used in all the experiments are summarized in Table 1.

4. Results and discussion

4.1. Resin characteristics

Physico-chemical parameters of the resin were determined according to procedures described in Section 3.2 and are listed in Table 2. FT-IR spectroscopy was used for identifying the functional group complexed with metal ions, the shift or absence of certain bands in the resin matrix as well as the presence of new bands. Fig. 1 shows FT-IR spectra of original and conditioned resin samples, as well as resin loaded with metal. The appearance of bands near 1730 and 1220 cm^{-1} is caused by the stretching vibrations of the carbonyl groups (C=O). The first band is not observed in the spectrum c) probably due to the involvement of the group in the chelation of the metal. The bands near 1390 cm^{-1} may be attributed to $-COO^-$ groups. There are no significant differences between the spectra corresponding to original and conditioned resins. It should be noted that only the band characteristic of C=O and COO^- groups (1217 and 1392 cm^{-1}) in spectrum a) were slightly shifted to higher frequencies (1219 and 1396 cm^{-1}) after the resin conditioning (spectrum b)), thus indicating the effect of the washings with HCl/NaOH. The band near 1100 cm^{-1} is absent in the spectra shown in Fig. 1 suggesting that the nitrogen atom in the imino

Table 2
General characteristics and properties of resin.

Item	Property
Functional group	$-N(CH_2COOH)_2$
Structure	Chelating-type
Ionic form	H
Particle size distribution (μm) [3]	300–1000
Apparent density (g dry resin cm^{-3})	0.425
Wet density (g wet resin cm^{-3})	1.015
Moisture content (%)	58.0
Wet particle porosity	0.657

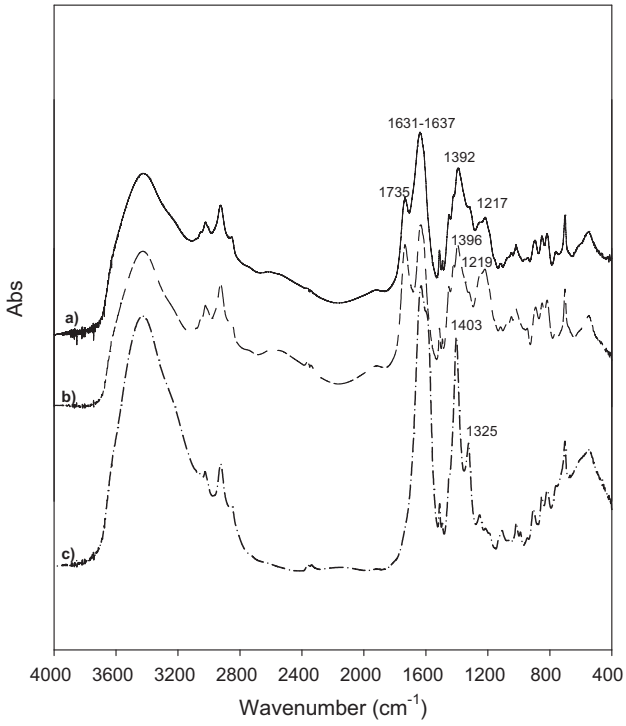

Fig. 1. IR spectra of original (a), conditioned (b) and loaded (c) resin.

Table 3
Experimental conditions and equilibrium parameters of Eq. (5) for the binary system Cu^{2+}/H^+.

Run	Initial conditions			Parameters calculated	
	pH	Concentration (meqv L^{-1})	Temperature (°C)	q_{max} (meqv g^{-1})	$K_{M,H}$
1	2	8	25	0.86	2.45
2	3	8	25	1.30	2.45
3	5	8	25	2.01	2.45
4	3	8	50	2.20	3.40

group is still protonated under pH conditions tested. Finally, the band 702 cm^{-1} deals with the presence of aromatic groups in the matrix which were not affected by the metal complexation [29–31].

4.2. Equilibrium studies

This study aims to investigate the effects of initial pH, metal concentration and temperature on ion-exchange equilibrium data for the binary system Cu^{2+}/H^+. The sorption of trivalent chromium into Diaion CR 11 resin is described elsewhere [32]. The starting conditions for each experiment (pH and metal concentration), the temperature (kept constant along the experiment) and the equilibrium parameters (q_{max} and $K_{M,H}$) are shown in Table 3. The parameters, q_{max} and $K_{M,H}$, were determined by fitting the equilibrium model, Eq. (5), to experimental the data by shifting them iteratively in order to minimize the average deviation, AD (%), calculated according to the equation:

$$AD = \frac{1}{N}\sum_{1}^{N}\left|\frac{Y_M^{exp,i} - Y_M^{cal,i}}{Y_M^{exp,i}}\right| \times 100 \quad (23)$$

where $Y_M^{exp,i}$ and $Y_M^{cal,i}$ are the experimental and calculated ionic fractions of metal in the solid phase, respectively. In most of cases, those deviations were less than 12% leading to a satisfactory fit of the equilibrium data to the model as shown in Figs. 2 and 4–6.

For trivalent chromium, Cavaco et al. [32] reported values of sorption capacity q_{max} of 0.29 at 25 °C and 0.66 meqv g^{-1} at 50 °C with solutions at initial pH approximately of 3.3. A higher sorption capacity (0.62 meqv g^{-1}) at 25 °C, using other commercial lot of Diaion CR 11 resin, was found by Gando-Ferreira et al. [33]. As shown in Table 3, q_{max} values obtained for Cu^{2+} at 25 °C were 0.86, 1.30 and 2.01 meqv g^{-1} for initial pH values of 2, 3 and 5, respectively. These experimental values are higher than the minimum one indicated by the resin manufacturer (0.73 meqv g^{-1}) [22]. In the literature, some works report exchange capacities for copper and chromium using other chelating resins containing iminodiacetate group. For Amberlite IRC 748, capacity values of 0.018 for Cr_t and 3.34 meqv g^{-1} for Cu^{2+} were observed by Janin et al. [8]. Gode and Pehlivan [12] found maximum sorption capacities for trivalent chromium of 1.023 and 0.86 meqv g^{-1} of Cr_t for Lewatit TP 207 and Chelex 100 at pH of 4.5. These data shows clearly that the different sorption capacities previously indicated depend on the experimental conditions, mainly of the pH solution. Indeed, the dissociation degree of the iminodiacetic acid is affected by the pH, being that at low pH the capacity resin decreases because there are few acid groups dissociated.

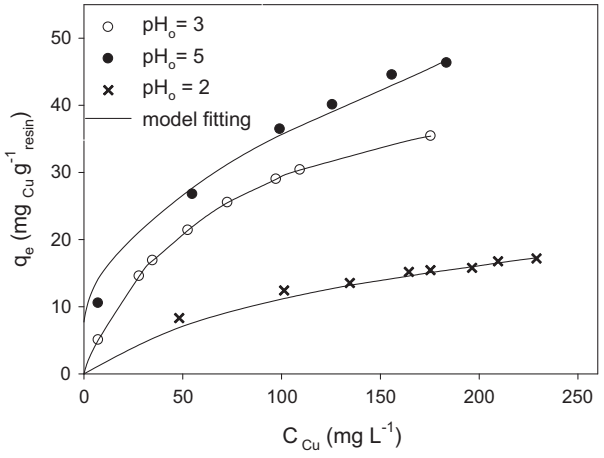

Fig. 2. Effect of initial pH on ion-exchange equilibrium data for the binary system Cu^{2+}/H^+, at 25 °C.

Comparing the values of q_{max} for copper with those previously referred for Cr^{3+}, it can be concluded that the Diaion CR 11 resin shows a major preference for copper than for chromium. The higher selectivity of the resin towards Cu^{2+} is a key issue for the selective separation of both metals in the case of treatment of industrial effluents. Indeed, a solution of high purity of trivalent chromium can be recovered for reuse during the saturation step of the ion exchange process.

4.2.1. Effect of initial pH

In general, the pH has strong influence on the amount of metal ions exchanged due to the competition with hydrogen ions for the binding sites of the resin, and usually sorption is favored at high initial pH. In the case of Diaion CR 11, the resin contains iminodiacetic groups anchored to the styrene divinyl-benzene chains and its complexing tendency is similar to ethylenediaminetetraacetic acid (EDTA). Due to the presence of carboxylic acid groups the resin may be classed as a weak acid cationic exchange resin whose apparent capacity in terms of exchangeable counter ions is dependent on the solution pH. However, it should be emphasized the high selectivity of this resin type, which forms stable coordination covalent bonds with divalent metals, when compared to ordinary exchangers. The structure of a weak acid cationic resin with respect to the iminodiacetic group is dependent on the solution pH. In general, it is fully protonated at pH below ~2 and acid groups exist as $-CH_2COOH$. At pH between 2 and 4, the resin is composed of functional groups $-CH_2COOH$ and $-CH_2COO^-$. The complete ionization of the groups occurs at pH ~ 7.4 [34]. Therefore, for the pH range tested, the exchange between metal ions and resin leads to the releasing of 1 proton, as described by Eq. (2).

The effect of initial pH on the exchange capacity of Diaion CR 11 resin is shown in Fig. 2. In fact, according to the results reported in Table 3, the maximum capacity, q_{max}, increased 2.3 times when the pH changed from 2 to 5 at 25 °C. At pH 5, the percentage of metal in solution removed ranged between 33% and 97% with increasing amounts of resin ranging between 0.07 and 1.0 g. The percentage of metal removed was between 9% and 83% for an initial pH of 2. The variation of the distribution coefficient of Cu^{2+} ($D = \rho_h q_e/C$) with pH is illustrated in Fig. 3 and can be seen that the maximum sorption capacity is achieved at pH around 5. In fact, the D value increased from 94 $cm^3_{sol}\ cm^{-3}_{resin}$ at pH 2 to about 495 $cm^3_{sol}\ cm^{-3}_{resin}$ at pH 5 for the conditions indicated in the legend of Fig. 3. Considering the solubility product of $Cu(OH)_2$, K_{ps}, equal to 2.2×10^{-20} at 25 °C [35], it is worth mentioning that for a copper concentration of 8 meqv L^{-1}, the initial pH of the solution should not be higher than approximately 5.4 to avoid the precipitation of metal hydroxide salt.

The pH of the solution decreased during the exchange of metal ion on resin for all experiments. In fact, the pH variation (ΔpH) was more pronounced in the experiment with an initial pH of 5 due to higher metal uptake by the resin. It was observed that ΔpH changed from 2.4 to 2.0 units over the range 7–184 mg L^{-1} of copper solution, under equilibrium conditions. Clearly, those lower ΔpH values are associated to the higher final concentrations of metal ion in solution which is due to the lower exchanges between metal and hydrogen

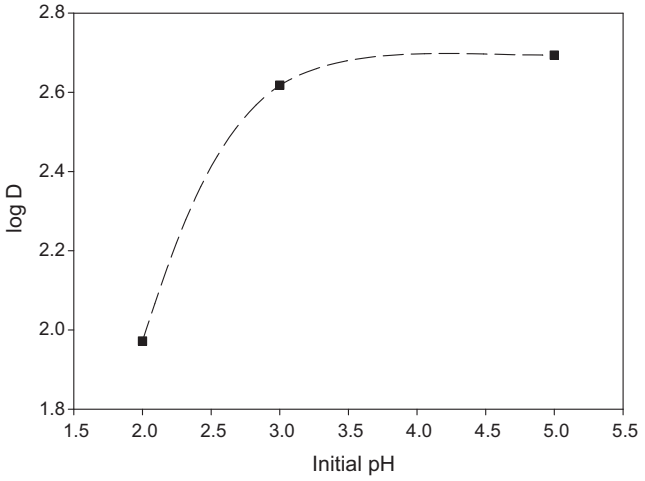

Fig. 3. Effect of initial pH on the distribution coefficient of Cu^{2+} on Diaion CR 11 (resin mass = 0.3 g; $C_{initial}$ = 8 meqv L^{-1}; solution volume = 40 mL; T = 25 °C).

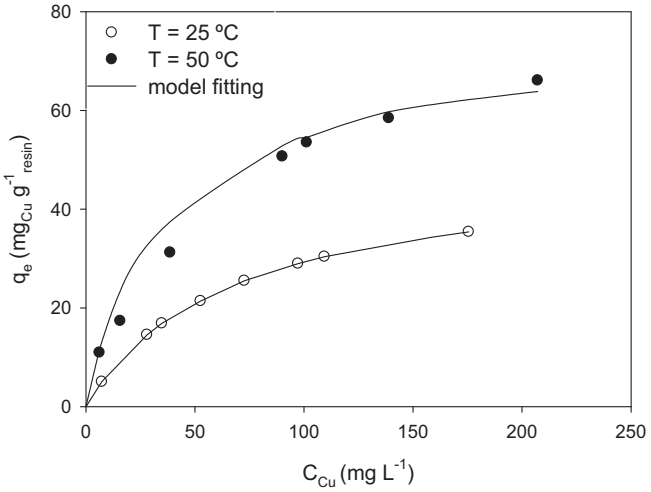

Fig. 5. Effect of temperature on ion-exchange equilibrium for the system Cu^{2+}/H^+ at initial pH 3.

ions of the resin. It is important to notice that, although the initial pH affects the maximum capacity of the resin for the metal ion, the equilibrium constant, $K_{M,H}$, remains unchanged, as expected (see Table 3). All the experimental points obtained at different initial pH fall on a single line as shown in Fig. 4, and as aforementioned, this line was obtained by fitting Eq. (5) to the experimental data, being the adjustable parameters $K_{M,H}$ and q_{max}. In the diagram Y vs X plotted in Fig. 4, the favorable nature of the ion-exchange process for the system tested, when $K_{M,H}$ = 2.45, leads to a curve located above of the diagonal.

4.2.2. Effect of temperature

The effect of temperature was studied by determining equilibrium data at 25 and 50 °C for an initial pH of 3. The results are shown in Figs. 5 and 6, where it can be observed that the retention of metal increases at higher temperatures. The effect of this variable on the separation factor, $K_{M,H}$, can be interpreted under the general thermodynamic relationship:

$$\frac{d \ln K_{M,H}}{dT} = \frac{\Delta H^0}{RT^2} \tag{24}$$

where T is the temperature, R the universal gas constant and ΔH^0 the enthalpy of exchange. Considering that ΔH^0 is independent of temperature, Eq. (24) can be integrated to give

$$\ln K_{M,H} = C^* - \frac{\Delta H^0}{R}\frac{1}{T} \tag{25}$$

where C^* is an integration constant. The formation of a chelate, between metal ion and iminodiacetic group of the resin, leads to a significant positive change in entropy, ΔS^0, of the ion-exchange process [36]. This means that the variation of Gibbs free energy, ΔG^0, with the temperature should be negative ($\Delta G^0 = \Delta H^0 - T\Delta S^0$). Therefore, ΔG^0 becomes more negative as the temper-

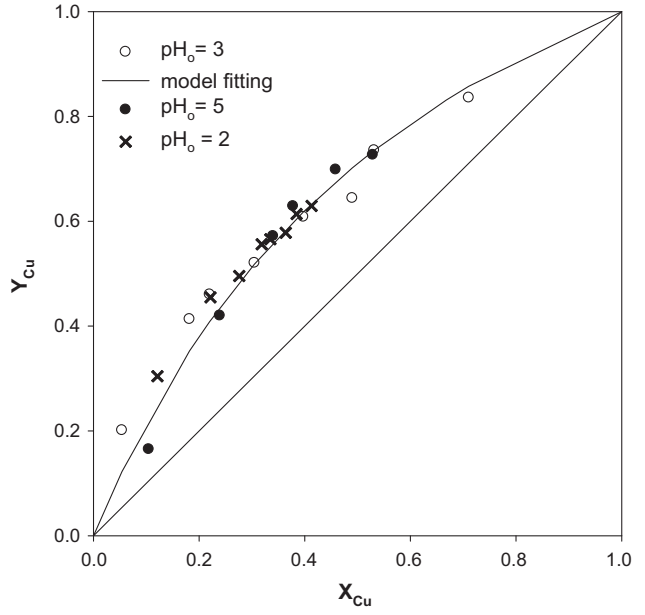

Fig. 4. Ionic fraction of copper in the solid phase as a function of the ionic fraction observed in the liquid phase.

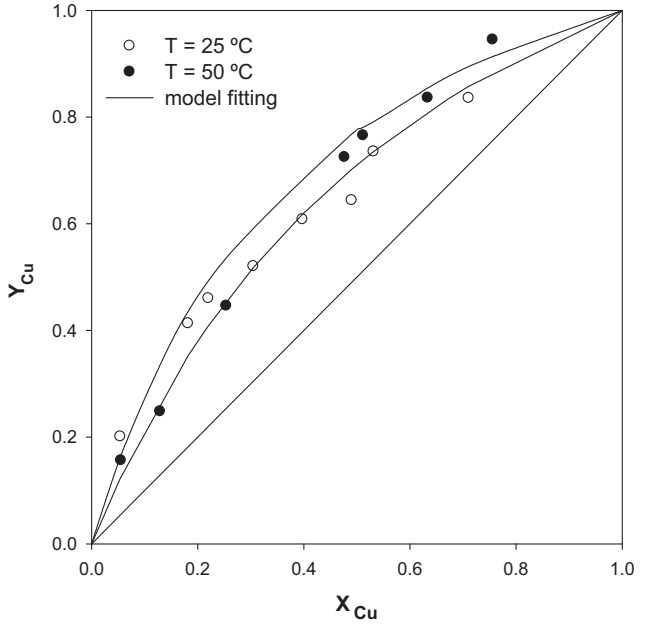

Fig. 6. Effect of temperature on ionic fraction of metal in the solid phase as a function of the ionic fraction observed in the liquid phase for the system Cu^{2+}/H^+ at initial pH 3.

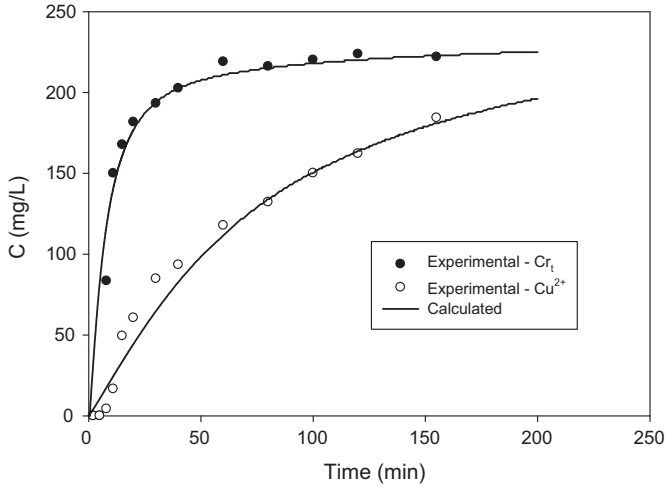

Fig. 7. Experimental and simulated sorption breakthrough curves for Cr_t and Cu^{2+} – Run 1.

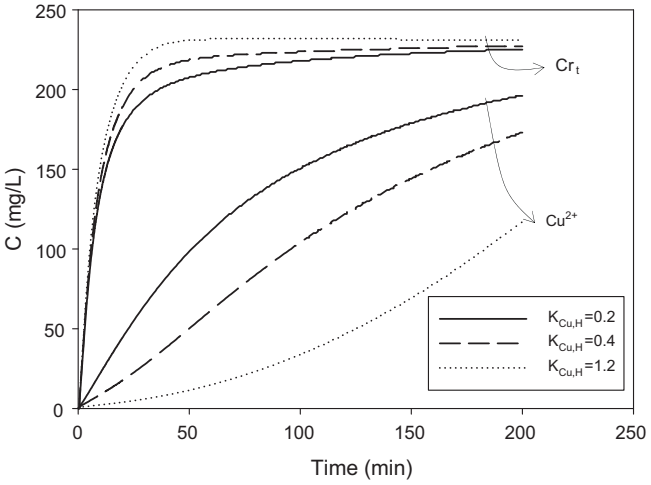

Fig. 9. Effect of equilibrium constant for the binary system Cu^{2+}/H^+ on the breakthrough curves of copper and chromium.

ature increases and thus higher separation factors are obtained under these conditions. The experimental results indicate that $K_{M,H}$ increased 1.4 times when the temperature rises from 25 to 50 °C. Fitting the experimental data to Eq. (25), a ΔH^0 of 11 kJ mol^{-1} was estimated. Consequently, the ion-exchange reaction between Cu^{2+} and Diaion resin is an endothermic process, which is favored as the temperature increases. It was also found that the maximum exchange capacity increases with the temperature probably due to its effect on the deprotonation degree of the carboxylic groups associated to the iminodiacetic acid of the resin [36].

4.3. Saturation and regeneration column breakthrough analysis

Fixed bed experiments were carried out under conditions reported in Table 1, for studying the dynamic behavior of the sorption process of copper and chromium onto the resin Diaion CR 11, as well as the elution of the metals from the resin using suitable regenerant agents. Experimental and simulated breakthrough curves plotted as metal concentration at column outlet against time are illustrated in Figs. 7 and 8. The saturation curves of copper and chromium show that Cu^{2+} ion emerges later since this metal is strongly adsorbed by the resin, confirming thus the equilibrium studies. In addition, it is clear that greater inlet cooper concentrations lead to a faster saturation of the resin with that metal. This is due to the fact that at higher concentrations, the isotherm gradient is lower (the kinetic constant, K_{LDF_i}, is high in Eq. (11), yielding a higher driving force along the pores). Hence, the equilibrium is attained faster for values of higher solute concentration. The behavior of the saturation curve of chromium is slightly affected by the change of copper concentration feed. The column test corresponding to Run 1 (Fig. 7) showed that the total uptakes for Cr_t and Cu^{2+} were 0.36 and 0.87 meqv g^{-1}, respectively. For Run 2 (Fig. 8) those values were of 0.28 and 0.81 meqv g^{-1}. In the first case, it was reached 95% of total capacity of the resin, q_{max}, whereas that in the second one was achieved 62% of q_{max}. This lower percentage value for the resin's uptaking capacity (for both metals) deals with the higher time needed for reaching the bed saturation with copper as shown in Fig. 8.

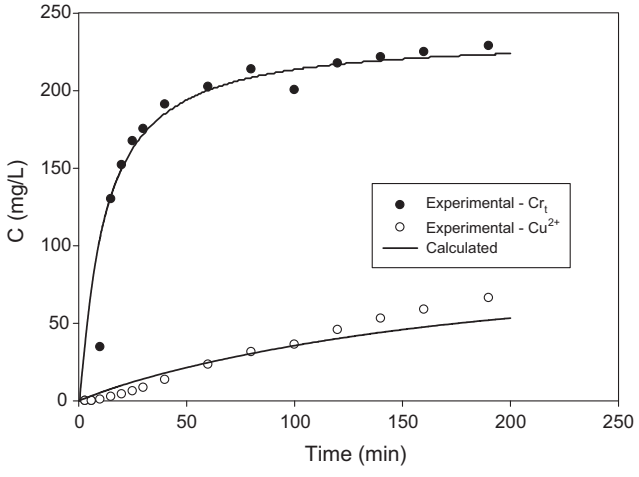

Fig. 8. Experimental and simulated sorption breakthrough curves for Cr_t and Cu^{2+} – Run 2.

The model was successfully fitted to the experimental outlet concentration data for both metals by using the following parameter values: $K_{Cr,H} = 0.05$, $K_{Cu,H} = 0.2$ and $D_{eCr,t} = 2.19 \times 10^{-10}$ m^2 s^{-1}. The estimated equilibrium constant for the binary system Cu^{2+}/H^+, $K_{Cu,H}$, is substantially lower than those calculated in the equilibrium studies at initial pH 3. This discrepancy can be justified considering the effect of the competition between the two metals, as well as the influence of total concentration on the resin's selectivity. At high concentrations, the selectivity may be influenced by phenomena such as ionic-pair formation, uncompleted solvated ions and accumulation of co-ions within the resin [37]. The saturation experiments were performed with initial concentration of metal ions in the feed solution that may occur in some industrial effluents of electroplating processes and whose values are higher concentration than in the solutions tested for determining equilibrium data. It is known that in the presence of a greater total concentration of cations, the resin exhibits lower selectivity, and this effect can change the favorable nature of isotherm to unfavorable depending on the order of magnitude of those concentrations [38].

Fig. 9 exhibits the sensitivity analysis of the system under analysis in respect to the equilibrium constant, $K_{Cu,H}$. As shown in this figure, increasing $K_{Cu,H}$ causes higher breakthrough time for the copper species resulting in a better separation of the two metals.

The experimental elution curves for Cu^{2+} and Cr_t plotted against the time, at different operating conditions, are shown in Figs. 10–14. The regeneration method was carried out in a sequential way using HCl followed of the mixture $NaOH/H_2O_2$. The use of the oxidation step with peroxide hydrogen in the presence of sodium hydroxide enables to overcome the difficulties of stripping triva-

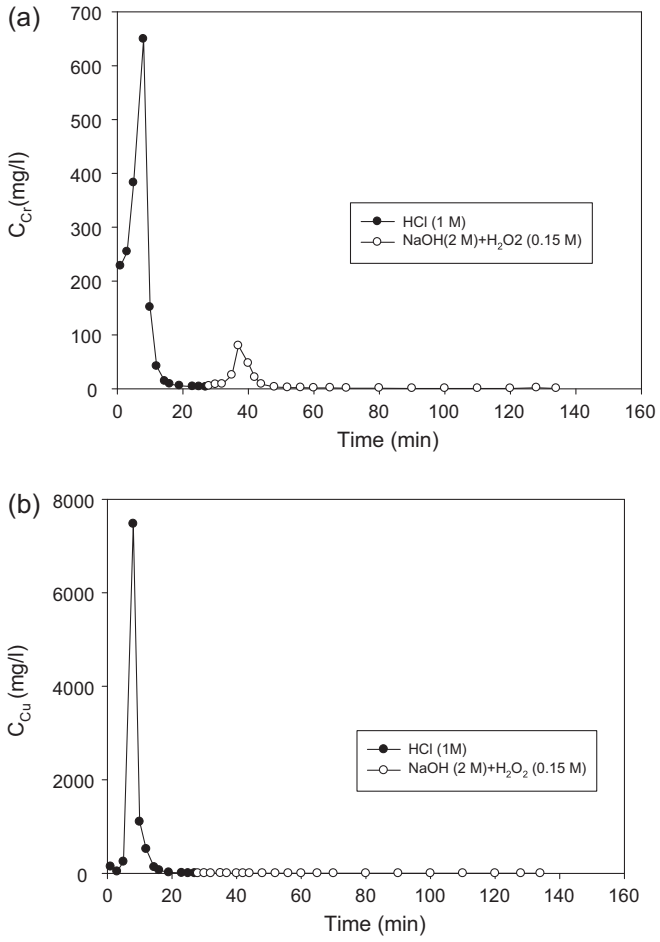

Fig. 10. Regeneration curves for (a) Cr_t and (b) Cu^{2+} with HCl (1 M) and NaOH (2 M)/H_2O_2 (0.15 M) at T = 25 °C – Run 3.

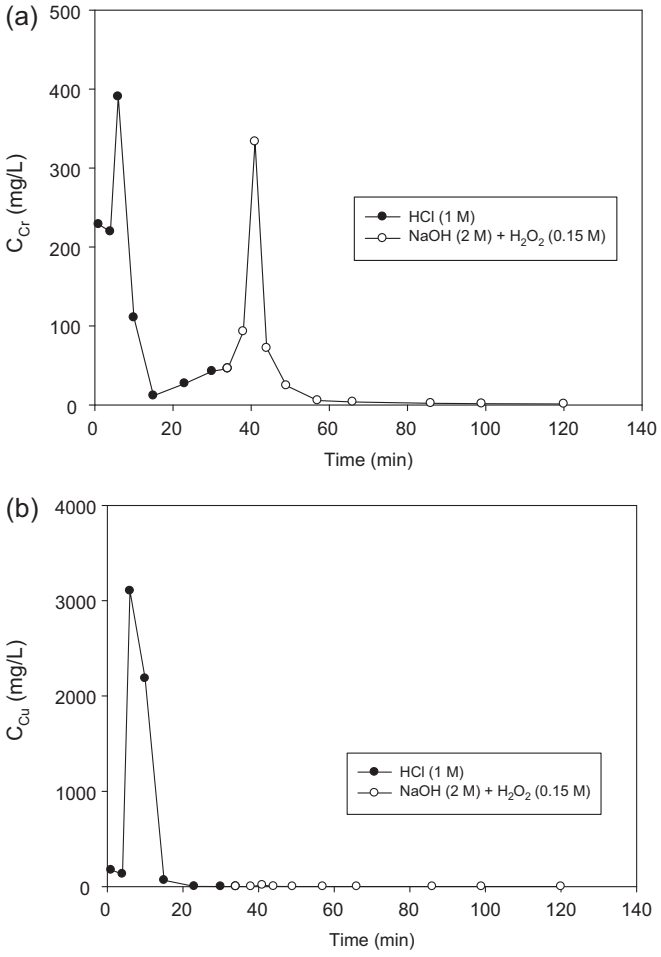

Fig. 11. Regeneration curves for (a) Cr_t and (b) Cu^{2+} with HCl (1 M) and NaOH (2 M)/H_2O_2 (0.15 M) at T = 50 °C – Run 4.

lent chromium from cationic resins. The oxidation reaction occurs as follows:

$$2Cr^{3+} + 3H_2O_2 + 10OH^- \rightarrow 2CrO_4^{2-} + 8H_2O \quad (26)$$

as a result, there is formation of the anionic specie CrO_4^{2-} which is rejected by the resin. The results illustrated in Figs. 10 and 11 were obtained by keeping the regeneration concentrations constant (HCl 1 M and NaOH 2 M/H_2O_2 0.155 M) at two different temperatures. In Fig. 10(a), the elution curve for Cr_t reached a concentration peak 2.8 times higher than the feed concentration (230 mg L^{-1}) used during the resin saturation after elution with 4 BV (1 BV ≈ 20 cm^3) of HCl. For copper, Fig. 10(b), the concentration peak corresponds to a concentration factor of 33 orders of magnitude in comparison with the feed concentration (230 mg L^{-1}). Regeneration efficiencies of 60.9 and 9.5% were found for chromium during the first and second elution steps. Copper is completely striped from the resin with HCl in which almost 100% (99.7%) of regeneration efficiency was achieved.

The regeneration behavior of the resin is affected by the temperature. The factor concentration of chromium in the peak of the elution curve was approximately of 1.7 with 3 BV of HCl and 1.5 after elution with 3.5 BV of NaOH/H_2O_2 as can be seen in Fig. 11(a). Regarding copper, a factor concentration of 13.5 was determined by using 3 BV of HCl, Fig. 11(b). At 50 °C the regeneration process is less efficient due to higher affinity of the resin for both metals as the temperature increases. The chromium was stripped from the resin with overall efficiencies of 70 and 65% at 25 °C and 50 °C, respectively, whereas for copper the efficiency decreased from 99.7% to 87.3%. Despite the increase in temperature does not favor the Cr_t elution, the comparison of results shown in Figs. 10(a) and 11(a) supports the conclusion that to operate at 50 °C may be advantageous to recover chromium. In fact, during the second regeneration step, Fig. 11(a), a concentrated solution of chromium with high purity may be collected at column outlet for reuse.

The elution curves shown in Fig. 12 were obtained for a more concentrated solution of hydrogen peroxide (0.3 M). The overall regeneration efficiency for chromium was improved under these conditions, increasing from 65.1% to 71.6%. This improvement can be justified considering that the oxidation of trivalent chromium to the hexavalent form is affected by the H_2O_2 concentration, as demonstrated by Kamel et al. [39]. This work reports that the oxidation reaction follows a first order kinetics in which the logarithm of the rate constant varies linearly with log [H_2O_2]. However, if the hydrogen peroxide exceeds the stoichiometric value, the oxidation process is not favored due to the disproportionation reaction of H_2O_2 ($H_2O_2 \rightarrow H_2O + 1/2O_2$) [21].

In order to increase the effectiveness of the regeneration process for chromium, additional experiments were performed exploiting the presence of iron. Indeed, it is known that the trivalent chromium oxidation rate by H_2O_2 can be increased in the presence of some transition metals such as Co^{2+}, Ni^{2+} and Fe^{3+} that act as catalysts. Fig. 13 compares the elution behavior of the resin pre-saturated with 464 mg L^{-1} of Cr_t in the absence and presence of iron (16.4 mg L^{-1}). Overall regeneration efficiencies of 72.5% and 96.5% were obtained for the solution without and with iron, respectively. In the case where iron is used, the concentration factor of chromium

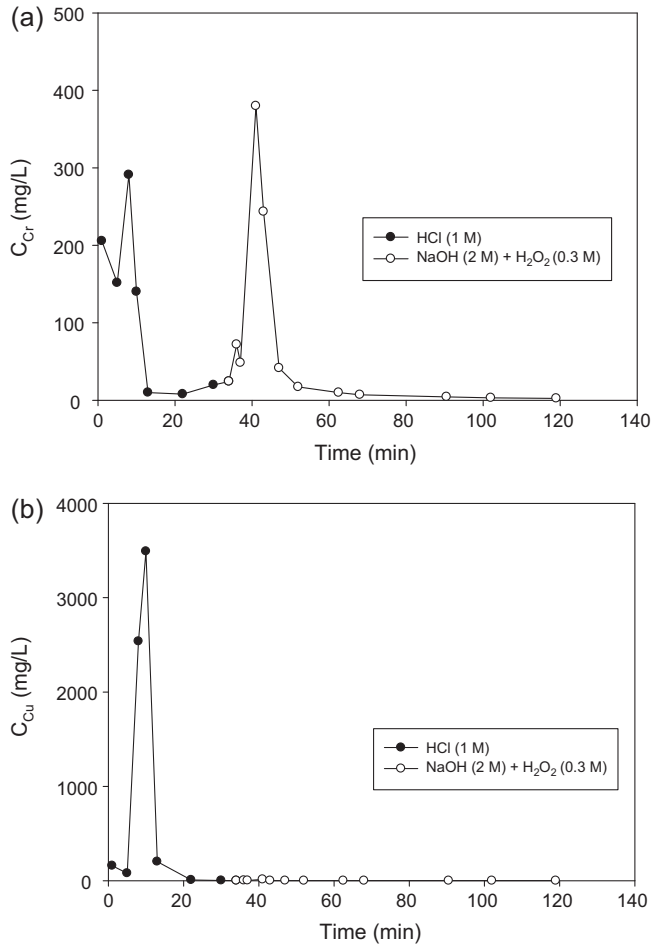

Fig. 12. Regeneration curves for (a) Cr_t and (b) Cu^{2+} by using HCl (1 M) and NaOH (2 M)/H_2O_2 (0.30 M) solutions at T = 50 °C – Run 5.

in the peak of the elution curve was of 2 with 3 BV of HCl and 1.8 after elution with 4 BV of NaOH/H_2O_2.

As aforementioned in Section 1, there is little literature on the regeneration studies for chelating resins loaded with metals and especially involving trivalent chromium. For the chelating resin Dowex M4195 with bis-picolyamine as functional group, Janin et al. [8] reported that 94% of copper and 81% of chromium were eluted from the resin using NH_4OH (4 M). The effluent treated by this resin

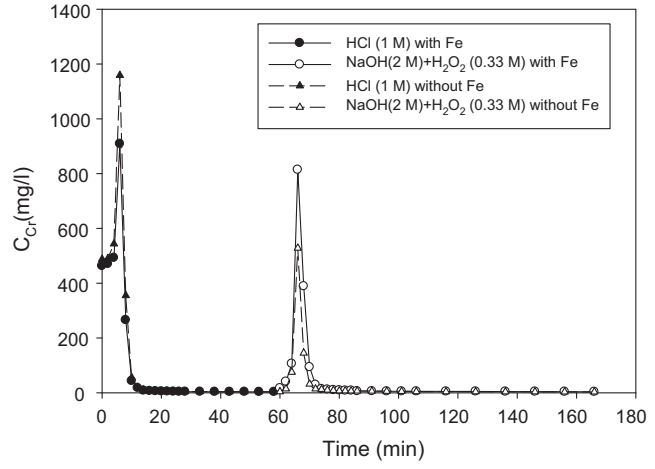

Fig. 13. Effect of presence of iron on the regeneration curves of chromium – Run 6.

was composed of 530 mg L^{-1} Cr, 456 mg L^{-1} Cu and 7.3 mg L^{-1} Fe. For the carboxylic resin Purolite C106 used for treating a wastewater containing approximately 160 mg L^{-1} of Cr and 50 mg L^{-1} of Al, Petruzzelli et al. [21] demonstrated that 95% of trivalent chromium was eluted with the mixture 0.15 M H_2O_2/1 M NaOH. However, in both cases was not possible to recover a non-contaminated solution of chromium for reuse as achieved through the regeneration approach investigated in our work.

5. Conclusions

The chelating ion-exchange resin Diaion CR 11, in the hydrogen form, was tested for removing Cr^{3+} and Cu^{2+} from synthetic effluents. The equilibrium isotherms showed that the resin has a stronger affinity for copper ions than to chromium ions. An ion-exchange equilibrium model was able to satisfactorily correlate the experimental data of the binary system Cu^{2+}/H^+. It was found that the maximum adsorption capacity is increased with the initial pH of the solution, whilst the equilibrium constant ($K_{Cu,H}$) value remains constant. It was also demonstrated that $K_{Cu,H}$ increases 1.4 times when the temperature changes from 25 °C to 50 °C. Moreover, the maximum exchange capacity increases with the temperature according to the endothermic nature of the ion-exchange process.

The breakthrough curves, obtained by the saturation operations in column with synthetic solutions, allowed studying the dynamic behavior of the process for the multicomponent system $Cu^{2+}/Cr_t/H^+$. The mathematical model used to simulate the breakthrough curves takes into account the axial dispersion for the liquid phase and linear driving force (LDF) for intraparticle mass transfer. The model simulates well the experimental data, and therefore, it can be used as a suitable approach for the design of industrial systems directed to the treatment of effluents from electroplating processes.

The regeneration process of the resin was carried out in a sequential way by using a HCl solution followed by a mixture of NaOH/H_2O_2. The regeneration efficiencies for both metals are affected by the temperature and peroxide hydrogen concentration. High efficiencies were obtained for copper during the first step, where this metal is almost completely eluted from the resin with 1 M HCl. The regeneration protocol based on elution with HCl and NaOH/H_2O_2, in the presence of iron, seems to be a good solution for effectively striping chromium from the resin.

Nomenclature

AD	average deviation, %
C	solute concentration in the fluid phase, mg L^{-1}
d_p	particle diameter, cm
D_{ax}	axial dispersion coefficient, $cm^2\ s^{-1}$
D_e	effective diffusivity, $cm^2\ s^{-1}$
D_m	molecular diffusivity, $cm^2\ s^{-1}$
$K_{M,H}$	equilibrium constant involving metal M
K_{LDF_i}	linear driving force kinetic constant, s^{-1}
L	bed length, cm
Pe	axial Peclet number ($=uL/\varepsilon D_{ax}$)
Q	flow rate, $cm^3\ s^{-1}$
q_i	adsorbed concentration of species i in equilibrium conditions, meqv $g^{-1}_{wet\ resin}$
q_{max}	maximum adsorption capacity (Langmuir parameter), meqv $g^{-1}_{wet\ resin}$
Re	Reynolds number ($=u\rho d_p/\mu\varepsilon$)
R_p	particle radius, cm
t	time, s
T	temperature, °C
u	bed superficial velocity, $cm\ s^{-1}$
u^*	normalized radial coordinate (r/R)

x dimensionless solute concentration in the bulk liquid phase (C/C_E)
X_p equivalent fractions for each species in liquid phase (C_i/C_T)
X_p dimensionless solute concentration in the liquid inside pores (C_p/C_E)
Y_i equivalent fractions for each species in solid phase (q_i/q_{max})
z bed axial coordinate, m
z^* normalized axial coordinate (z/L)

Greek letters
ε bed porosity
ε_p particle porosity
ΔH^0 enthalpy of exchange, kJ mol^{-1}
ΔG^0 Gibbs free energy, kJ mol^{-1} K^{-1}
λ equivalent ionic conductance
ρ density of the fluid, g cm^{-3}
ρ_h wet density of the adsorbent, g cm^{-3}
θ normalized time (t/τ)
μ viscosity of the fluid, g cm^{-1} s^{-1}
τ space time, s
τ_p tortuosity

Subscripts
i species i
E inlet conditions
j species j
o initial
T total

Acknowledgements

We would like to thank FCT (Foundation for Technology and Science) for its financial support for this work (Project POCTI/EQU/58149/2004). The authors would like also to thank the assistance provided by Paulo Alexandre Alves and Pedro Nuno Pereira fifth-year students in Chemical Engineering at the University of Coimbra.

References

[1] Z.L. He, X.E. Yang, P.J. Stoffella, Trace elements in agroecosystems and impacts on the environment, J. Trace Elem. Med. Biol. 19 (2005) 125–140.
[2] P.K. Rai, Heavy metal phytoremediation from aquatic ecosystems with special reference to macrophytes, Crit. Rev. Environ. Sci. Technol. 39 (2009) 697–753.
[3] S.A. Cavaco, S. Fernandes, C.M. Augusto, M.J. Quina, L.M. Gando-Ferreira, Evaluation of chelating ion-exchange resins for separating Cr(III) from industrial effluents, J. Hazard. Mater. 169 (2009) 516–523.
[4] C. Cervantes, J. Campos-Garcia, S. Devars, F. Gutierrez-Corona, H. Loza-Tavera, J.C. Torres-Guzman, R. Moreno-Sanchez, Interactions of chromium with microorganisms and plants, FEMS Microbiol. Rev. 25 (2001) 335–347.
[5] A.K. Shanker, C. Cervantes, H. Loza-Tavera, S. Avudainayagam, Chromium toxicity in plants, Environ. Int. 31 (2005) 739–753.
[6] K.V. Brix, D.K. DeForest, W.J. Adams, Assessing acute and chronic copper risks to freshwater aquatic life using species sensitivity distributions for different taxonomic groups, Environ. Toxicol. Chem. 20 (2001) 1846–1856.
[7] P. Babula, V. Adam, R. Opatrilova, J. Zehnalek, L. Havel, R. Kizek, Uncommon heavy metals, metalloids and their plant toxicity: a review, Environ. Chem. Lett. 6 (2008) 189–213.
[8] A. Janin, G. Mercier, P. Drogui, Selective recovery of Cr and Cu in leachate from chromated copper arsenate treated wood using chelating and acidic ion exchange resins, J. Hazard. Mater. 169 (2009) 1099–1105.
[9] C.-Y. Chen, M.-S. Lin, K.-R. Hsu, Recovery of Cu(II) and Cd(II) by a chelating resin containing aspartate groups, J. Hazard. Mater. 152 (2008) 986–993.
[10] E. Pehlivan, T. Altun, Ion-exchange of Pb^{2+}, Cu^{2+}, Zn^{2+}, Cd^{2+}, and Ni^{2+} ions from aqueous solution by Lewatit CNP 80, J. Hazard. Mater. 140 (2007) 299–307.
[11] L.-C. Lin, R.-S. Juang, Ion-exchange kinetics of Cu(II) and Zn(II) from aqueous solutions with two chelating resins, Chem. Eng. J. 132 (2007) 205–213.
[12] F. Gode, E. Pehlivan, A comparative study of two chelating ion-exchange resins for the removal of chromium (III) from aqueous solution, J. Hazard. Mater. B100 (2003) 231–243.
[13] F. Gode, E. Pehlivan, Removal of chromium (III) from aqueous solutions using Lewatit S 100: the effect of pH, time, metal concentration and temperature, J. Hazard. Mater. B136 (2006) 330–337.
[14] N. Kabay, N. Gizli, M. Demircioğlu, M. Yüksel, A. Jyo, K. Yamabe, T. Shuto, Cr (III) removal by macroreticular chelating ion exchange resins, Chem. Eng. Commun. 190 (2003) 813–822.
[15] S. Kocaoba, G. Akcin, Removal and recovery of chromium and chromium speciation with MINTEQA2, Talanta 57 (2002) 23–30.
[16] S. Kocaoba, G. Akcin, Removal of chromium (III) and cadmium (II) from aqueous solutions, Desalination 180 (2005) 151–156.
[17] S. Yalçin, R. Apak, J. Hizal, H. Afşar, Recovery of copper (II) and chromium (III,VI) from electro-plating industry wastewater by ion exchange, Sep. Sci. Technol. 36 (2001) 2181–2196.
[18] N. Kabay, M. Demircioğlu, H. Ekinci, M. Yüksel, M. Sağlam, M. Akçay, M. Streat, Removal of metal pollutants (Cd(II) and Cr(III)) from phosphoric acid solutions by chelating resins containing phosphonic or diphosphonic groups, Ind. Eng. Chem. Res. 37 (1998) 2541–2547.
[19] S.K. Sahu, P. Meshram, B.D. Pandey, V. Kumar, T.R. Mankhand, Removal of chromium(III) by cation exchange resin, Indion 790 for tannery waste treatment, Hydrometallurgy 99 (2009) 170–174.
[20] S. Rengaraj, K.H. Yeon, S.H. Moon, Removal of chromium from water and wastewater by ion exchange resins, J. Hazard. Mater. B87 (2001) 273–287.
[21] D. Petruzzelli, R. Passino, G. Tiravanti, Ion Exchange process for chromium removal and recovery from tannery wastes, Ind. Eng. Chem. Res. 34 (1995) 2612–2617.
[22] Diaion—Manual of Ion Exchange Resins and Synthetic Adsorbent, 2nd ed., Mitsubishi Chemical Corporation-Separation Materials, 1995.
[23] C.F. Baes, R.E. Mesmer, The Hydrolysis of Cations, John Wiley, New York, 1976.
[24] M.Z.M. Otero, M. Minceva, M. Zabka, A. Rodrigues, Separation of synthetic vanillin at different pH onto polymeric adsorbent Sephabeads SP06, Chem. Eng. Process. 45 (2006) 598–607.
[25] J.B. Butt, Reaction Kinetics and Reactor Design, 2nd ed., CRC Press, 2000, p. 350.
[26] N. Wakao, J. Smith, Diffusion in catalyst pellets, Chem. Eng. Sci. 17 (1962) 825–832.
[27] R.A. Robinson, R.H. Stokes, Electrolyte Solutions, 2nd ed., Butterworths, 1959.
[28] N. Madsen, R. Sincovec, PDECOL: general collocation software for partial differential equations, ACM Trans. Math. Software 5 (1979) 326–351.
[29] P. Ling, F. Liu, L. Li, X. Jung, B. Yin, K. Chen, A. Li, Adsorption of divalent heavy metal ions onto IDA-chelating resins: simulation of physicochemical structures and elucidation of interaction mechanisms, Talanta 81 (2010) 424–432.
[30] E.S. Dragan, M.V. Dinu, G. Lisa, A.W. Trochimczuk, Study on metal complexes of chelating resins bearing iminodiacetate groups, Eur. Polym. J. 45 (2009) 2119–2130.
[31] C. Xiong, C. Yao, Synthesis, characterization and application of triethylenetetramine modified polystyrene resin in removal of mercury, cadmium and lead from aqueous solutions, Chem. Eng. J. 155 (2009) 844–850.
[32] S.A. Cavaco, S.L. Fernandes, M.M. Quina, L.M. Gando-Ferreira, Removal of chromium from electroplating industry effluents by ion-exchange resins, J. Hazard. Mater. 144 (2007) 634–638.
[33] L.M. Gando-Ferreira, M.J. Quina, R. Quinta-Ferreira, Equilibrium and kinetics modelling of separation of Cr(III)/Cu(II) by a chelating resin from industrial effluents, in: Proc. CHEMPOR'2008, Portugal, 2008 (CD-ROM).
[34] Z. Zainol, M.J. Nicol, Ion-exchange equilibria of Ni^{2+}, Co^{2+}, Mn^{2+} and Mg^{2+} with iminodiacetic acid chelating resin Amberlite IRC 748, Hydrometallurgy 99 (2009) 175–180.
[35] R.H. Perry, D. Green, Perry's Chemical Engineers' Handbook, 6th ed., Mc-Graw Hill Chem. Eng. Series, 1984.
[36] F. Gode, Removal of chromium ions from aqueous solutions by the adsorption method, in: A.A. Lewinsky (Ed.), Hazardous Materials and Wastewater: Treatment, Removal and Analysis, Nova Science Publishers, Inc., New York, 2007, pp. 275–308.
[37] M.J. Jansen, A.J. Straathof, L.A. van der Wielen, K.C. Luyben, W.J. van den Tweel, Rigorous model for ion exchange equilibria of strong and weak electrolytes, AIChE J. 47 (1998) 1911–1924.
[38] M. Trgo, J. Perié, N. Vukojevié-Medvidovié, The effect of concentration and pH on selectivity of ion-exchange in system natural zeolite-Na^+/Zn^{2+} aqueous solutions, Stud. Surf. Sci. Catal. 158 (2005) 1051–1055.
[39] M. Kamel, F. Mijangos, M.P. Elizalde, Oxidative treatment for the prevention of chromium accumulation in a polymeric matrix, Solv. Extr. Ion Exchange 20 (2002) 575–588.